



Fermi National Accelerator Laboratory

FERMILAB-Pub-90/114-A  
May 1990

**CHIRAL INTERFACE  
AT THE FINITE TEMPERATURE  
TRANSITION POINT OF QCD**

Z. Frei<sup>†</sup>

NASA/Fermilab Astrophysics Center  
Fermi National Acceleratory Laboratory  
Box 500, Batavia IL 60510-0500

and

A. Patkós<sup>†</sup>

CERN, Theory Division  
1211 Geneva 23  
Switzerland

**ABSTRACT**

The domain wall between coexisting chirally symmetric and broken-symmetry regions is studied in a saddle-point approximation to the effective three-flavour  $\sigma$ -model. In the chiral limit the surface tension varies in the range  $[(40 - 50)\text{MeV}]^3$ . The width of the domain wall is estimated to be  $\simeq 4.5$  fm.

---

<sup>†</sup> On leave from Dept. of Atomic Physics, Eötvös University, Budapest, Hungary.



1. Recently, considerable effort has been invested into the determination of the surface tension between the low- and the high-temperature phases of quantum chromodynamics at the coexistence point [1,2]. These investigations have made use of the quenched lattice version of QCD. Already at modest temperature-extension of the lattice ( $N_t = 4$ ) considerable difficulties were met in extracting a reliable signal for the presence of the interface. In the full theory, the simulation of the phase transition with 4 light flavours is well under control [3]. In the phenomenologically more interesting  $N_f = 2, 3$  cases the order of the transition is not settled yet [4,5].

On the basis of these remarks the renewal of interest in the effective low energy theories of QCD seems to be justified in the present context too. Since some exploratory investigations indicate that near the phase transition the high temperature phase of QCD might also be described in terms of colourless, massive excitations [6], there is a chance that the phase transition itself can be understood fully in this framework.

In this Letter we present a semiquantitative analysis of the interface between coexisting chirally symmetric and broken symmetry regions in a three-flavour linear  $\sigma$ -model.

The most successful effective meson model is based on the non-linear realisation of the broken-symmetry vacuum [7,8]. In particular, based on the observation that the finite-temperature partition function of QCD is determined at low  $T$  by the Goldstone sector, an expansion has been derived for the quark condensate,  $\langle \bar{\psi}\psi \rangle$  to  $O(T^6)$  [9]. A smooth extrapolation of its decreasing tendency towards higher  $T$  indicates that the restoration of chiral symmetry would take place at  $\approx 170$  MeV for  $N_f = 2$ . In view of the possible first-order nature of the transition this is rather an upper bound on  $T_c$ . As such, it is in agreement with the results of MC-simulations of the full QCD with two [10] and four [3] light flavours (in the latter case the proportionality of  $T_c$  to  $N_f^{-1/2}$  is to be taken into account). However, a fully conventional approach to the chiral phase transition within the non-linear model is prevented by the absence of an explicit order parameter field in this theory. Actually, this field is traded for the coupling  $F_\pi$ , whose temperature-variation has been also studied in the literature [9,11].

An interesting variant of this low-energy description incorporates also a glueball field, fulfilling the trace anomaly already at the tree level [12,13,14]. The resulting idea of a unique mechanism for the finite temperature variation of the

chiral and gluon condensates has been investigated recently in Ref.[15].

It is in the linear  $\sigma$ -model where the scalar singlet order parameter field appears explicitly. Although the existence of the scalar nonet is a notoriously disputed subject, recent analyses claim, that by taking into account the existence of  $K-\bar{K}$  molecules, a nonet with the appropriate features can be proposed uniquely [16]. The linear model at the tree level represents equally well the low-energy meson sector as the non-linear version [17,18,19]. However, it has been explicitly shown that renormalisation is not the correct way to improve its predictions [20]. Therefore, it is a reasonable strategy [21] to estimate the modification of the tree-level potential at finite temperature by taking into account exclusively the thermal fluctuations.

This “classical” interpretation of the effective model has been implemented in Ref.[21] by simply omitting the  $T$ -independent (divergent) part of the one-loop finite temperature quantum correction of the effective potential. This certainly cannot be considered a consistent approach. Instead, we emphasize that the  $\sigma$ -model provides a classical field-theoretical model for the ground state of QCD, which can be investigated at finite temperature in the framework of classical statistical physics. We remark that recently the role played in the deconfinement by skyrmions has been investigated in the  $SU(2) \times SU(2)$  non-linear model with the same philosophy [22]. Before proceeding to the construction of the chiral order parameter profile, we shall calculate the constrained free energy [23,24] of the tree-level parametrized linear  $\sigma$ -model as for a classical field theory at finite temperature. A first-order transition will be detected for  $N_f = 3$  in agreement with the results of the general renormalisation group analyses [25,26]. Once the functional form of the free energy constrained by the constant non-zero value of the  $\sigma$ -field is calculated at  $T_c$  numerically, the construction and the analysis of the chiral order parameter profile goes along the same lines as earlier for the Polyakov-loop profile [27].

The present approach is in full analogy with the treatment of magnetism with the help of classical spin-models (Ising, Heisenberg etc.), where the quantal nature of the magnetic phenomena is reflected only in the actual value of the nearest neighbour, etc. couplings calculated at zero temperature. The applicability of such models to real magnetic crystals depends on the success or failure of their predictions. The same statement applies to the content of the present note.

2. The Hamiltonian of the linear  $\sigma$ -model is given by

$$\begin{aligned}\mathcal{H}[M] &= \frac{1}{2} \int d^3x \operatorname{tr} \Pi^2 + \mathcal{H}_P[M], \\ \mathcal{H}_P[M] &= \int d^3x \left[ \frac{1}{2} \operatorname{tr} (\nabla M)(\nabla M^\dagger) - \frac{\mu_0^2}{2} \operatorname{tr} M M^\dagger + g(\det M + \det M^\dagger) \right. \\ &\quad \left. + f_1 (\operatorname{tr} M M^\dagger)^2 + f_2 \operatorname{tr} (M M^\dagger)^2 \right],\end{aligned}\quad (1)$$

where the complex matrix  $M$  represents the scalar ( $\sigma$ ) and the pseudoscalar ( $\phi$ ) nonets:

$$M(x) = \frac{1}{\sqrt{2}} \sum_{l=0}^8 (\sigma_l(x) + i\phi_l(x)) \lambda_l, \quad \operatorname{tr} \lambda_l \lambda_k = 2\delta_{lk}.\quad (2)$$

The matrix  $\Pi$  is formed from the conjugate momenta of  $M$ . In our concrete calculations we shall make use of the parametrisation proposed by Goldberg [21], which leads to an  $SU(3)$ -symmetric spontaneous breaking of the  $SU(3) \times SU(3)$  chiral symmetry:

$$\mu_0 = 244\text{MeV}, \quad g = -1811\text{MeV}, \quad f_1 = 1.70, \quad f_2 = 11.91.\quad (3)$$

For the construction of the chiral profile the constrained free energy, corresponding to a non-zero fixed value of  $\bar{\sigma}_0(\mathbf{k} = \mathbf{0})$ , the  $\mathbf{k} = 0$  Fourier component of  $\sigma_0(x)$ , is the appropriate quantity to evaluate. After integrating over the conjugate momenta the partition function of the classical medium defined by Eq. (1) and Eq. (3) is given by

$$\begin{aligned}Z[\sigma_0] &\equiv \exp\{-\beta V \mathcal{U}(\sigma_0)\} \\ &= \int \mathcal{D}M \delta(\bar{\sigma}_0(\mathbf{k} = \mathbf{0}) - \sigma_0) \prod_{l=1}^8 \delta(\bar{\sigma}_l(\mathbf{k} = \mathbf{0})) \prod_{l=0}^8 \delta(\bar{\phi}_l(\mathbf{k} = \mathbf{0})) \exp\{-\beta \mathcal{H}_P\},\end{aligned}\quad (4)$$

where  $\beta = T^{-1}$ .

The integration over  $M$  in a finite volume  $V$  is done by separating the  $\mathbf{k} = 0$  mode explicitly:

$$M(x) = \frac{1}{\sqrt{3}} \sigma_0 I + m(x), \quad \bar{m}(\mathbf{k} = \mathbf{0}) = 0.\quad (5)$$

Reshuffling Eq. (1) accordingly, one proceeds to an approximate evaluation of the  $m$ -integral, which would be exact in an infinite component model (actually, here

one has 18 components). First, an auxiliary  $3 \times 3$  matrix field  $\Sigma(x)$  is introduced, which formally transforms the quartic piece in the exponent of Eq. (4) into one which is quadratic in  $m$ . Next, one assumes that the  $\Sigma$ -integration is dominated by an  $SU(3)$ -symmetric saddle-point:

$$\Sigma(x) = \hat{s} I. \quad (6)$$

Third, one performs the  $m$ -integration in the Gaussian approximation, which yields the leading low-temperature correction to the zero-temperature free energy. (The perturbation theory with respect to the cubic piece of  $\mathcal{H}_P$  corresponds to a loop expansion, where the role of  $\hbar$  is played by  $\beta^{-1} = T$ .)

The detailed presentation of the above procedure can now be found in textbooks [28], therefore we directly give the infinite-volume result for the one-loop correction of the constrained free energy, evaluated at the saddle point:

$$\frac{1}{V} \Delta \mathcal{U}_{saddle} = T \int \frac{d^3 k}{(2\pi)^3} \frac{1}{2} \sum_Q g(Q) \ln(k^2 + X(Q)). \quad (7)$$

In this equation the index  $Q$  runs over the scalar singlet (S0), the scalar octet (S8), the pseudoscalar singlet (P0), and the pseudoscalar octet (P8) meson-multiplets,  $g(Q)$  gives the corresponding multiplicities,  $X(Q) \equiv \hat{s} + \mu_0^2 + \mu^2(Q)$  acts as a kind of effective squared mass, while  $\mu^2(Q)$  at  $\sigma_0 = \sigma_{min}(T = 0)$  yields the meson masses in the chiral limit:

$$\begin{aligned} \mu^2(S0) &= -\mu_0^2 + \frac{4g}{\sqrt{3}}\sigma_0 + 4\sigma_0^2(3f_1 + f_2), & g(S0) &= 1, \\ \mu^2(S8) &= -\mu_0^2 - \frac{2g}{\sqrt{3}}\sigma_0 + 4\sigma_0^2(f_1 + f_2), & g(S8) &= 8, \\ \mu^2(P0) &= -\mu_0^2 - \frac{4g}{\sqrt{3}}\sigma_0 + \frac{4}{3}\sigma_0^2(3f_1 + f_2), & g(P0) &= 1, \\ \mu^2(P8) &= -\mu_0^2 + \frac{2g}{\sqrt{3}}\sigma_0 + \frac{4}{3}\sigma_0^2(3f_1 + f_2), & g(P8) &= 8. \end{aligned} \quad (8)$$

One has to emphasize that the original integrand of Eq. (4) is exponentially small for large field values, therefore the saddle-point approximation loses its sense when any single  $X(Q)$  becomes negative. In the symmetric phase the particle masses are defined at  $\sigma_0 = 0$ , where  $\hat{s}$  has the meaning of the common mass square of the parity partners. At zero temperature  $\hat{s} = -\mu_0^2$  (see below), which implies by

Eq. (3)  $\sigma_{min} = 115$  MeV leading to a  $SU(3)$ -symmetric spectrum (P8: 0, P0: 850 MeV, S8: 950 MeV, S0: 600 MeV). Thus, the saddle-point approach holds the promise for a unified description of both phases.

The saddle-point value of the free energy is found by minimising its expression as a function of  $\hat{s}$  for fixed  $\sigma_0$ :

$$\frac{\partial \mathcal{U}_{saddle}[\hat{s}, \sigma_0]}{\partial \hat{s}} = 0. \quad (9)$$

The formal procedure outlined above is given sense by applying a cut-off  $\Lambda$  on the  $k$ -integral in Eq. (7). This is physically natural, since the effective theory ceases to represent QCD, even approximately, when high-energy fluctuations start to play an important role. For the numerical calculations it is convenient to use scaled (dimensionless) quantities:

$$\begin{aligned} \tau &= \frac{T}{\Lambda}, & s &= \frac{\hat{s}}{\Lambda^2}, & \sigma &= \frac{\sigma_0}{\Lambda}, \\ \gamma &= \frac{g}{\Lambda}, & \bar{\mu}_0 &= \frac{\mu_0}{\Lambda}, & \bar{X} &= \frac{X}{\Lambda^2}. \end{aligned} \quad (10)$$

The cut-off integral of Eq. (7) was calculated analytically:

$$\begin{aligned} \mathcal{U}_{saddle}[s, \sigma, \Lambda] &= \Lambda^4 \left\{ -\frac{3}{8(3f_1 + f_2)} \left( \frac{1}{2}s^2 + s\bar{\mu}_0^2 \right) - \frac{1}{2}\bar{\mu}_0^2\sigma^2 + \frac{2}{3\sqrt{3}}\gamma\sigma^3 + \left( f_1 + \frac{1}{3}f_2 \right) \sigma^4 \right. \\ &\quad \left. + \frac{\tau}{12\pi^2} \sum_Q g(Q) [\ln(1 + \bar{X}(Q)) + 2\bar{X}(Q) - 2\bar{X}(Q)^{3/2} \arctan \bar{X}^{-1/2}(Q)] \right\}. \end{aligned} \quad (11)$$

The explicit expression of Eq. (9) can be obtained by taking the partial derivative of Eq. (11) with respect to  $s$ .

Eq. (9) has been solved for several values of  $\Lambda$  in the range  $\Lambda \in (250, 2000)$  MeV. For each  $\Lambda$ ,  $\tau$  was varied and  $s(\Lambda, \tau, \sigma)$  found. In the range  $\Lambda \in (500, \approx 1000)$  MeV for some  $\sigma$ -values no saddle-point fulfilling the  $X > 0$  condition could be found. In these points the proposed approximation scheme fails. Based on the  $T_c$ -range of lattice-calculations discussed in the introduction, our strategy was to choose values of  $\Lambda$  tuning the critical temperature over the interval  $T_c \in (100, 200)$  MeV. It turns out that the interesting interval in this sense is  $\Lambda < 400$  MeV, where the saddle-point approximation works well.

Evaluating Eq. (11) at the saddle point, at very low  $\tau$  its double-well nature inherited from the classical potential is preserved. When increasing  $\tau$ , the position

of the non-trivial minimum shifts considerably towards the symmetric minimum at the origin. The degeneracy of the corresponding potential values occurs before their locations coincide. In the whole parameter region, where the saddle-point approximation makes sense, a clean first-order transition was observed. It is worth mentioning that on both sides of the transition temperature we found physical values for the saddle point ( $X > 0$ ), which can be contrasted with the case of continuous phase transitions, discussed in [28], where the critical point is identified from the symmetric phase as the end of the validity of the saddle-point dominance.

In Fig. 1 we illustrate the typical evolution of the potential with the temperature for  $\Lambda = 300\text{MeV}$ . Other values of the cut-off lead only to quantitative changes. In Fig. 2 the smooth variation of  $T_c$  with  $\Lambda$  is displayed. Although  $T_c < \Lambda$  in the whole range, the relevant  $\Lambda$  values are lower than what is intuitively expected. We remark that  $T_c \leq 10\text{MeV}$  for  $\Lambda \geq 1\text{GeV}$ .

3. When the critical temperature is fixed by choosing  $\Lambda$ , no free parameter remains in the theory. The complete characterisation of the chiral interface will be given in physical units. The kink equation

$$\frac{d^2 \sigma_0}{dx^2} = \frac{d \mathcal{U}(\sigma_0)}{d\sigma_0} \quad (12)$$

is discretised using a lattice constant ( $a$ ) proportional to  $\Lambda^{-1}$

$$x = la, \quad a = \frac{1}{n\Lambda}, \quad n = 1, 2, \dots \quad (13)$$

The discretised equation for the dimensionless quantities was solved in the form

$$\sigma(l+1) = 2\sigma(l) - \sigma(l-1) + \frac{1}{n^2\Lambda^4} \frac{d \mathcal{U}_{saddle}}{d\sigma}. \quad (14)$$

The kink solution of the  $\Lambda = 300\text{ MeV}$  case suggests very slight  $n$ -dependence, even for  $n = 1, 2$  (Fig. 3). In addition, we have calculated the surface tension,

$$\frac{\alpha}{\Lambda^3} = \sum_l \left[ \frac{1}{2} n (\sigma(l) - \sigma(l-1))^2 + \frac{1}{n\Lambda^4} \mathcal{U}_{saddle}(\sigma) \right] \quad (15)$$

which also shows very slight  $n$ -dependence. In Table 1 we give the surface tension ( $\alpha$ ), the width of the interface ( $d$ ) and the value of the non-trivial  $\sigma_{min}$  at  $T_c$  for a few  $T_c$ -values from the relevant range. The most important observation is that

none of them seem to be particularly sensitive to  $T_c$ . The results summarized in the Abstract are rather robust.

The range of  $\alpha$  found by us is almost one order of magnitude smaller than the bag-model estimate of Ref.[29]. Although Campbell *et al.* have given some support to that result in their effective model calculation, our thickness estimate sheds some doubt on the validity of the thin-wall approximation used in [15]. This wall-thickness of 4–5 fm is a somewhat intriguing result of the present study. It would mean that in heavy ion collisions, in a large part of the fireball only a decrease of the quark-condensate could be achieved, as the tail of the surrounding low-temperature vacuum enters fairly deep into the high energy-density region. Such a situation might motivate the study of particle emission from states intermediate between the fully broken and the symmetric phases at  $T_c$ .

Our additional numerical investigation showed that if the mass of the scalar singlet is increased by up to 950 MeV (the other parameters are kept fixed) no quantitative change occurs in the characteristics of the interface. However, if the mass of the whole scalar sector is larger (of the order of 1.5 GeV) the surface tension would grow to the value conjectured in Refs. [32], and its width would decrease to 2 fm.

4. In this investigation we have attempted a semi-quantitative characterisation of the chiral interface at the QCD phase transition point. The linear  $\sigma$ -model was just a choice, where the temperature dependent corrections to the free energy density of the  $\sigma$ -field could be estimated. The model certainly has to be extended to take into account further light degrees of freedom with significant coupling to  $\sigma$ . A first step in this direction could be a model incorporating an additional glueball-field [14]. We note, that with careful discretisation, which takes into account the essential role played by the cut-off, one can use non-perturbative lattice methods for the study of the thermodynamics of low-energy effective theories as well.

### Acknowledgements

In the course of forming their approach the authors benefited from conversations with J. Gasser, P. Hasenfratz, H. Leutwyler and F. Niedermayer. We thank F. Karsch for many useful comments on the manuscript. Z. F. acknowledges the support of the DoE and the NASA (through grant NAGW-1340), the NSF at the University of Chicago, and thanks the hospitality of the Astrophysics Group at Fermilab. This work also appeared as CERN preprint: CERN-TH.5745/90.

## References

- 1) K. Kajantie, L. Kärkkäinen and K. Rummukainen, Nucl. Phys. B333 (1990) 100.
- 2) S. Huang, J. Potvin, C. Rebbi and S. Sanielevici, Boston preprint BUHEP-89-34, January 1990.
- 3) R.V. Gavai, S. Gupta, A. Irbäck, F. Karsch, S. Meyer, B. Petersson, H. Satz and H.W. Wyld, CERN-TH-5530/89.
- 4) M. Fukugita, H. Mino, M. Okawa and A. Ukawa, Tsukuba-preprint, UTHEP-204, April 1990.
- 5) J.B. Kogut and D.K. Sinclair, Illinois preprint, ILL-(TH)-90-7, March 1990.
- 6) C.E. DeTar and J.B. Kogut, Phys. Rev. D36 (1987) 2828.
- 7) H. Leutwyler, Nucl. Phys. (Proc. Suppl.) 7A (1989) 42.
- 8) J. Gasser, Bern preprint BUTP-89/27, (to appear in Proc. of Cargese Summer School: Hadrons and Hadronic Matter, 1989).
- 9) P. Gerber and H. Leutwyler, Nucl. Phys. 321B (1989) 387.
- 10) S. Gottlieb, W. Liu, R.L. Renken, R.L. Sugar, and D. Toussaint, Phys. Rev. D38 (1987) 2245.
- 11) A. Barducci, R. Casalbuoni, S. De Curtis, R. Gatto and G. Pettini, Geneva-preprint, UGVA-DPT 1990/01-647.
- 12) J. Ellis, Nucl. Phys. B22 (1970) 478.
- 13) J. Schechter, Phys. Rev. D21 (1981) 3393.
- 14) H. Gomm, P. Jain, M. Johnson and J. Schechter, Phys. Rev. D33 (1986) 801.
- 15) B.A. Campbell, J. Ellis and K.A. Olive, CERN-TH-5620/89
- 16) J. Weinstein, Univ. of Tennessee preprint, UTK-89-7, (to appear in Proc. of Int. Conf. on Hadron Spectroscopy, 22-27 Sept. 1989, Ajaccio).
- 17) J. Schechter and Y. Ueda, Phys. Rev. D3 (1971) 176.
- 18) P. Carruthers and R.W. Haymaker, Phys. Rev. D4 (1971) 1815.
- 19) L.H. Chan and R.W. Haymaker, Phys. Rev. D7 (1973) 402.
- 20) J. Gasser and H. Leutwyler, Ann. Phys. 158 (1984) 142.
- 21) H. Goldberg, Phys. Lett. 131B (1983) 133.
- 22) C.E. DeTar, Utah preprint, UUHEP-90/1.
- 23) R. Fukuda, Prog. of Theor. Physics 56 (1976) 258.
- 24) L. O'Raiheartaigh, A. Wipf and H. Yoneyama, Nucl. Phys. B271 (1986) 653.
- 25) R. Pisarsky and F. Wilczek, Phys. Rev. D29 (1984) 338.

- 26) A. Margaritis, G. Ódor and A. Patkós, Z. Phys. C39 (1988) 110.
- 27) Z. Frei and A. Patkós, Phys. Lett. B222 (1989) 469.
- 28) A.M. Polyakov, Gauge Fields and Strings (Harwood, 1987).
- 29) C. Alcock and E. Farhi, Phys. Rev. D32 (1985) 1273;  
G.M. Fuller, G.J. Mathews and C.R. Alcock, Phys. Rev. D37 (1988) 1380.

Table 1

The transition temperature and the characteristic data of the chiral order parameter profile in the chiral limit of the linear  $\sigma$ -model as a function of the cut-off.

$\Lambda$ [MeV]	$T_c$ [MeV]	$\alpha^{1/3}$ [MeV]	$d$ [fm]	$\sigma_{min}$ [MeV]
230	225.77	38.9	4.5	48.5
240	199.14	39.7	4.5	50.2
250	176.66	40.6	4.5	51.8
260	157.55	41.3	4.5	53.0
270	141.20	42.2	4.5	54.3
280	127.14	43.1	4.5	55.7
290	114.97	43.9	4.5	56.8
300	104.38	44.6	4.4	57.9
310	95.13	45.4	4.4	58.9
320	87.01	46.1	4.4	59.6

**Figure captions**

- Figure 1:** The variation of  $10^3 \times$  the scaled constrained free energy density vs. the scaled  $\sigma$ -field with the temperature. The curves, starting from below, correspond to  $T = 100$  MeV, 102 MeV,  $T_c$ , 106 MeV and 108 MeV, respectively.
- Figure 2:** The dependence of the critical temperature on the cut-off of the thermal fluctuations. Both  $T_c$  and  $\Lambda$  are measured in MeV.
- Figure 3:** The chiral order parameter profile displayed on a lattice with lattice constant  $a=1/3\Lambda$ . The different curves correspond to appropriately scaled-up kinks evaluated originally on lattices with  $a=1/\Lambda$  (solid),  $a=1/2\Lambda$  (dashed) and  $a=1/3\Lambda$  (dotted), respectively. The value of the  $\sigma$ -field is measured in MeV.

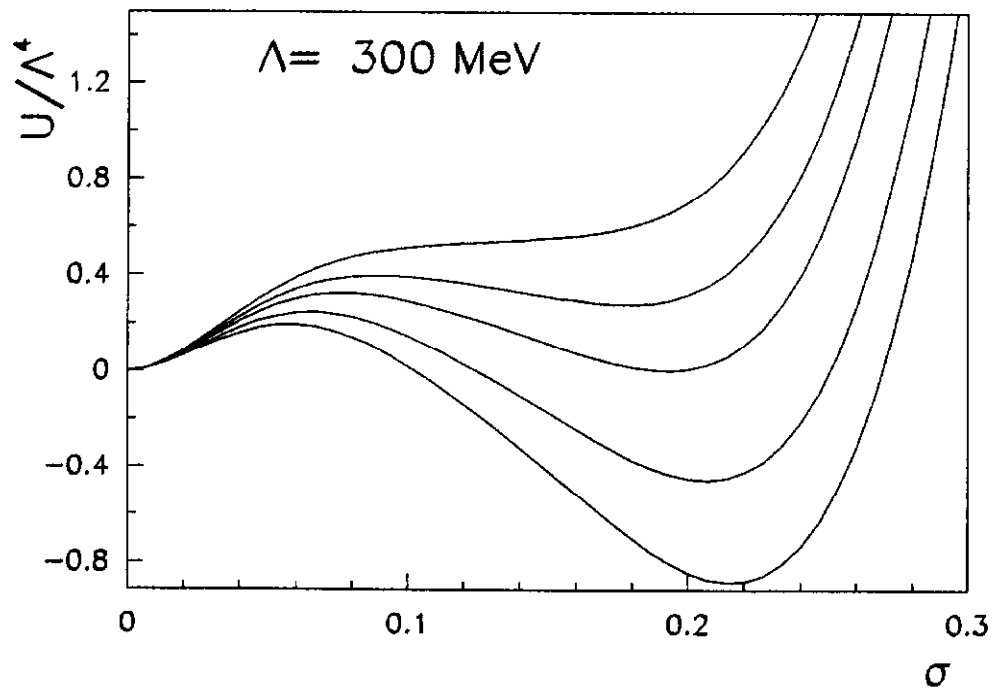


Figure 1

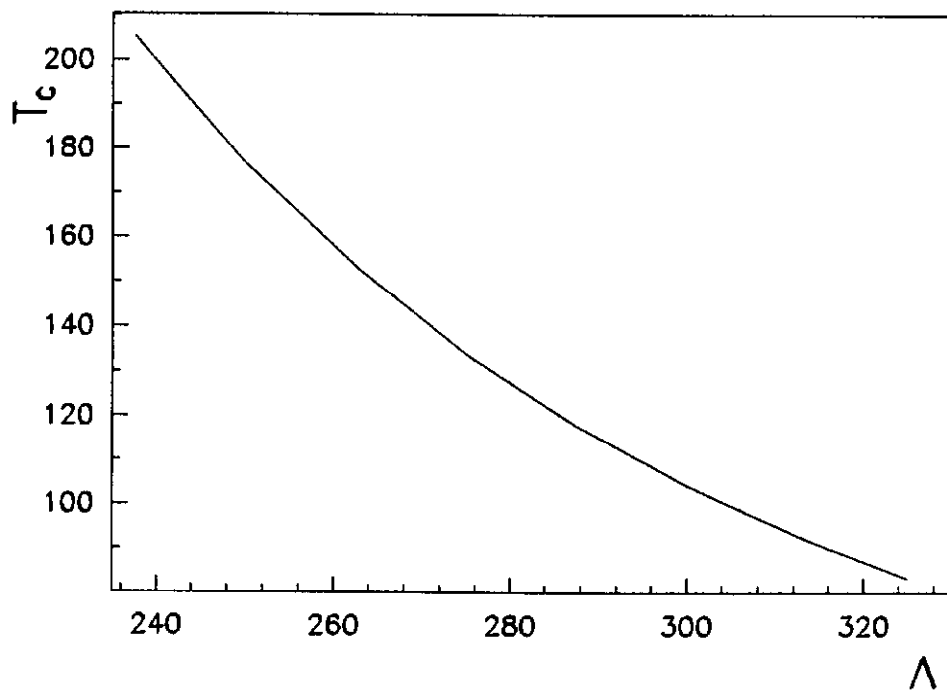


Figure 2

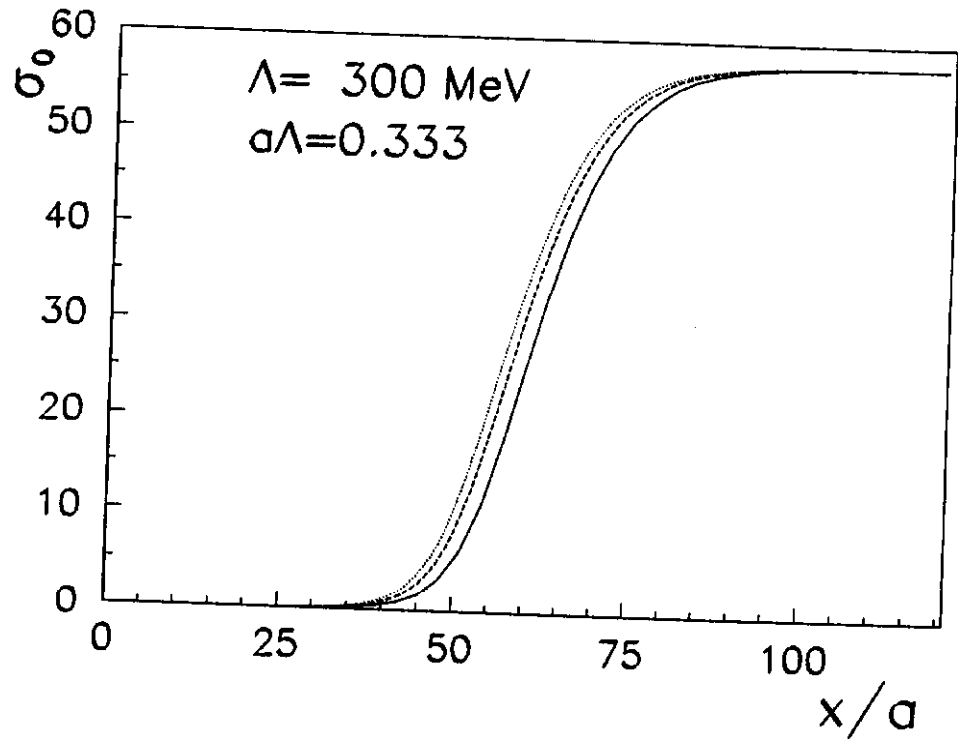


Figure 3